

## DYNAMICS OF THE HUMAN VOCAL CORDS

JAN AWREJCEWICZ

*Technical University of Łódź*

A systematic, global numerical analysis of the human vocal cords dynamics described in terms of the 5-th rang nonlinear differential equation system is presented in the paper. The state of equilibrium position of the vocal cords and the parameter space have been calculated first. By solving the boundary problem, the periodic trajectories creating by the equilibrium positions obtained from the Hopf bifurcation have been found next. The stability and possible bifurcations of the mentioned trajectories were followed by the observation the characteristic multipliers values variations. The influence of the parameters on periodic or quasiperiodic sound has been illustrated. The phenomenon of the register of a voice changes has been also discussed.

### 1. Introduction

This paper is based on a work of Cronjaeger [1], using extensive references given over there to help introducing a mathematical model of the human vocal cords. An important reference, in which the attempt to explain the phenomenon of voice production in the human larynx based on the myoelastic-aerodynamic theory has been given, belongs to Van der Berg [2-4] and Flanagan [5-8]. The human lungs produce a necessary air flow required for voice production. The air pressure causes a glottis to open. The glottis continues to open as a result of inertia until the elasticity of the vocal cords forces it to close. When the glottis closes, the airstream is expelled according to the Bernoulli suction effect and the pressure decreases. However, when the distance between the vocal cords is small enough, the vocal cords start to close as a result of inertial forces. Thus, the overpressure arises again and the above mentioned cycle of vibrations repeats.

The description of anatomy and physiology of the human larynx may be found in many works (c.f. Benninghoff-Goertteler [9], Lullies [10], Luchsinger [11] and Zöllner [12], Rohen, Tautz and Heckemann [13], Wustrow [14,15]). The myoelastic-aerodynamic theory which explains the production of sound was presented in various works by Van der Berg. Lullies, Lottermoser and Damste [16-18] showed that voice in the human larynx is produced analogously to some wind instruments rule

of action (haut-boy, clarinet, saxophone, accordion). Basing on these theoretical investigation, Cronjaeger formulated the nonlinear mechanical model describing the dynamics of the vocal cords. A model of the vocal cord was presented in his work as a two-degree-of-freedom nonlinear mechanical oscillator, consisting of an elastically supported point mass. The stiffness and damping characteristics of an anisotropic support of the mass correspond to real properties of the vocal cord. In order to describe the possibility of contact (impacts) of the vocal cords the additional elastic element (nonlinear spring) was used in the model. The stiffness of this element was chosen in such a way that for horizontal displacements of the mass approaching point 0 (in the given coordinate system) the force in the spring increases to infinity. Additionally, it is assumed that the air flow from the lungs is adiabatical and the Bernoulli effect is neglected. Lungs and air passage were modelled as a kettle with stiff walls. The real elastical properties of the lungs and air passage were additionally considered in the elastical properties of the air. The escaping air flow is proportional to the horizontal deflection of the vocal cords and to the flow rate of the air-stream in the kettle. Pressure in the kettle creates, approximately, identical forces both in the vertical and the horizontal directions of displacement of the vocal cords. Further details, concerning the construction of the model and the discussion of advantages and faults of it, are described by Cronjaeger. His mechanical model describing the dynamics of the vocal cords is governed by the fifth order system of nonlinear ordinary differential equations.

This paper aims at the systematical numerical approach to the study of the global behaviour of this system. The evolution of the system is traced by changing one freely chosen parameter. Beginning with the calculations of steady-state solutions the new periodic solutions which are born after Hopf bifurcation are discovered. Then, by tracing the evolution of the characteristic multipliers the changes of stability and the further bifurcation points are calculated. The paper focuses on the analysis of the equations of motion of the model in the space of parameters corresponding to those in the human larynx.

## 2. The mechanical model and the equations of motion

The lungs and the air-passage are modelled as a small kettle with the volume  $V$  (fig.1). The air flow  $q$  is introduced into this kettle. Using this model, Cronjaeger assumed that the volume of the vibrating lung is constant. The air from the kettle escapes passing through the vocal cords, which are modelled as two symmetric independent oscillators. The symmetric vibrations of the two oscillators are caused by air pressure. The coordinate system  $(x, y)$  describes horizontal and vertical displacements of the one of the oscillators. The equilibrium point for each of the oscillators is  $(x_0, 0)$ , and  $f$  is a distance between the centre of the mass and the

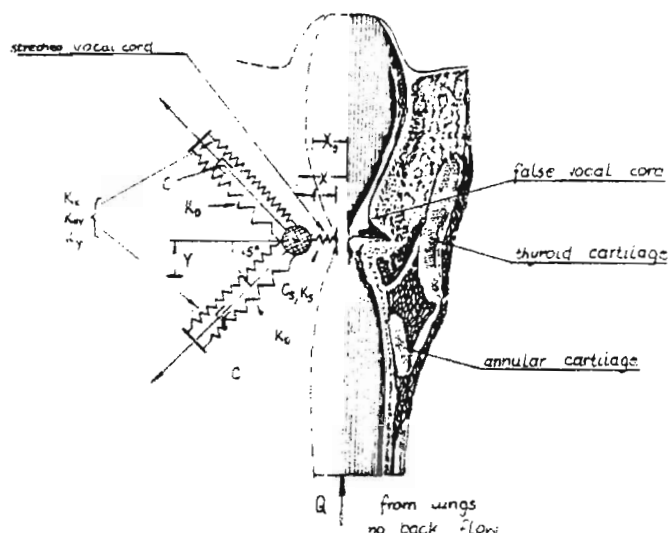


Fig. 1. Cross-section of larynx and the adequate mechanical model with marked dimensionless parameters (from Cronjaeger [1]).

edge of the vocal cord. The horizontal and vertical forces caused by air pressure are assumed to be equal. The air viscosity and inertia are neglected. On the basis of the assumptions presented above, Cronjaeger obtained the following system of equations governing the dynamics of the human vocal cords

$$\begin{aligned}
 m\ddot{x} + c\dot{x} + \{k_x + k_D[(x - x_0)^2 + y^2]\}(x - x_0) + \\
 -k_{xy}y - k_s x^{-s}(1 - c_s \dot{x}) &= \frac{1}{2}Ap, \\
 m\ddot{y} + c\dot{y} + \{k_y + k_D[(x - x_0)^2 + y^2]\}y - k_{xy}(x - x_0) &= \frac{1}{2}Ap, \quad (2.1) \\
 \dot{p} = \frac{\bar{p}\kappa}{\bar{\varphi}V} \begin{cases} \bar{\varphi}q - \frac{3}{4}\varphi_a k(x - f)\sqrt{\frac{2}{\varphi_a}p} & \text{for } x > f, \\ \bar{\varphi}q & \text{for } x \leq f, \end{cases}
 \end{aligned}$$

where:

- $m$  - mass of a vocal cord  $= 0.24 \cdot 10^{-3}$  kg,
- $c$  - damping of the vocal cord  $< 4 \cdot 10^{-4}$  Ns/m,
- $k_s$  - stiffness of the vocal cords (when brought together)  
 $< 0.1k_x f^{s+1}$ ,
- $k_x$  - horizontal stiffness of the vocal cord  $20 \div 2000$  N/m,
- $k_y$  - vertical stiffness of the vocal cord  $= (0.7 \div 0.9)k_x$ ,

- $k_{xy}$  - stiffness of the couplings between two directions of motion =  $(0.3 \div 0.5)k_x$ ,  
 $k_D$  - the Duffing type stiffness  $< 0.1c_x/f^2$ ,  
 $c_s$  - additional damping of the vocal cords (when brought together),  
 $s$  - exponent = 4,  
 $A$  - the vocal cord surface =  $6 \cdot 10^{-5} \text{ m}^2$ ,  
 $\bar{\varphi}$  - average subglottis air density =  $1.3 \text{ kg/m}^3$ ,  
 $\varphi_a$  - average atmosphere density =  $1.25 \text{ kg/m}^3$ ,  
 $\bar{p}$  - average subglottis pressure =  $1.01 \div 1.1 \text{ bar}$ ,  
 $h$  - length of the vocal cord =  $(12 \div 18) \cdot 10^{-3} \text{ m}$ ,  
 $f$  - distance from the point-mass to the edge of vocal cord =  $3 \cdot 10^{-3} \text{ m}$ ,  
 $\zeta$  - intensity of air flow  $< 6 \cdot 10^{-4} \text{ m}^3/\text{s}$ ,  
 $V$  - volume of the subglottis reservoir  $< 3 \cdot 10^{-3} \text{ m}^3$ ,  
 $\kappa$  - adiabata exponent = 1.4.

In order to obtain the dimensionless equations set, the following transformations are used:

$$\begin{aligned}
 t &= \frac{\tau}{\Omega}, & -\frac{d}{dt}(\dots) &= \bar{\Omega} \frac{d}{d\tau}(\dots) = \bar{\Omega}(\dots)', \\
 x(t) &= \bar{\alpha} X(\tau), \\
 y(t) &= \bar{\beta} Y(\tau), \\
 p(t) &= \bar{\mu} P(\tau).
 \end{aligned} \tag{2.2}$$

From eq.(2.1) we obtain:

$$\begin{aligned}
 X'' + \frac{b}{m\bar{\Omega}} X' + \left\{ \frac{k_x}{m\bar{\Omega}^2} + \frac{k_0}{m\bar{\Omega}^2} [\bar{\alpha}^2 (X - \frac{x_0}{\alpha})^2 + \bar{\beta}^2 Y^2] \right\} (X - \frac{x_0}{\alpha}) + \\
 - \frac{k_{xy}}{m\bar{\Omega}^2} \frac{\bar{\beta}}{\bar{\alpha}} Y - k_s \frac{\bar{\alpha}^{-s-1}}{m\bar{\Omega}^2} X^{-s} (1 - \bar{\alpha} C_s \bar{\Omega} X') = \frac{1}{2} \frac{A \bar{\mu} P}{\bar{\alpha} m \bar{\Omega}^2}, \\
 Y'' + \frac{b}{m\bar{\Omega}} Y' + \left\{ \frac{k_y}{m\bar{\Omega}^2} + \frac{k_0}{m\bar{\Omega}^2} [\bar{\alpha}^2 (X - \frac{x_0}{\alpha})^2 + \bar{\beta}^2 Y^2] \right\} Y + \\
 - \frac{k_{xy}}{m\bar{\Omega}^2} \frac{\bar{\alpha}}{\bar{\beta}} X = \frac{1}{2} \frac{A \bar{\mu} P}{\bar{\beta} m \bar{\Omega}^2}, \\
 p' = \frac{\kappa \bar{p}}{\bar{\Omega} V \bar{\mu}} q + \begin{cases} \frac{3}{4} \frac{\kappa \bar{p}}{\bar{\Omega} V \bar{\mu}} \frac{\rho_a}{\bar{\rho}} h \bar{\alpha} (X - \frac{L}{\alpha}) \sqrt{\frac{2}{\rho_a}} \bar{\mu} p & \text{for } X > \frac{L}{\alpha} \\ 0 & \text{for } X \leq \frac{L}{\alpha} \end{cases}
 \end{aligned} \tag{2.3}$$

Following relations are taken between the dimensional coefficients of the system (2.3)

$$\bar{\alpha} = \bar{\beta} = f,$$

$$\bar{\Omega}^2 = \frac{c_x}{m}, \quad (2.4)$$

$$\bar{\mu} = 2 \left( \frac{3}{4} \frac{\kappa \bar{p} h f}{r \hbar \omega \Omega V} \right)^2 \rho_a.$$

The new nondimensional coefficients are introduced in the way that

$$\begin{aligned} C &= \frac{b}{\sqrt{mk_x}}, \\ K_y &= \frac{k_y}{k_x}, \\ K_{xy} &= \frac{k_{xy}}{k_x}, \\ K_D &= \frac{k_D}{k_x} f^2, \\ X_0 &= \frac{x_0}{f}, \\ K_s &= \frac{k_s}{k_x} f^{-s-1}, \\ C_s &= f \frac{c_s}{\sqrt{mk_x}}, \\ E &= \frac{1}{2} \frac{A}{f k_x} \bar{\mu}, \\ Q &= \frac{\kappa \bar{p}}{V \bar{\mu}} q, \\ K_x &= \frac{k_x}{m \Omega^2} = 1. \end{aligned} \quad (2.5)$$

Finally, the dimensionless system of equations is obtained

$$\begin{aligned} \ddot{X} + C \dot{X} + \{K_x + K_D[(X - X_0)^2 + Y^2]\}(X - X_0) + \\ - K_{xy}Y - K_s X^{-s}(1 - C_s \dot{X}) = EP, \\ \ddot{Y} + C \dot{Y} + \{K_y + K_D[(X - X_0)^2 + Y^2]\}Y - K_{xy}(X - X_0) = EP, \\ \dot{P} = Q - \begin{cases} (X - 1)\sqrt{P} & \text{for } X > 1 \\ 0 & \text{for } X \leq 1 \end{cases}, \end{aligned} \quad (2.6)$$

where:

- $C$  - damping of the vocal cords  $< 1$ ,
- $K_y$  - vertical stiffness of the vocal cords (0.7, 0.9), (horizontal dimensionless stiffness is equal to 1),

- $K_{xy}$  - stiffness of the couplings between two directions of motion (0.1,...,0.5),
- $K_D$  - the Duffing type stiffness ( $< 0.01$ ),
- $K_s$  - stiffness of the vocal cords when brought together ( $< 0.01$ ),
- $S$  - exponent ( $= 4$ ),
- $C_s$  - damping of the vocal cords when brought together ( $< 1$ ),
- $X_0$  - the equilibrium point, position of cartilage, (0.1,...,0.2),
- $E$  - average pressure, the vocal cord surface (0.1,...,10),
- $Q$  - intensity of air-flow (0,...,100).

The vibrations of the vocal cords are governed by the nonlinear self-excited system of equations (2.6) with nine parameters. The presented intervals of the dimensionless variations of the parameters correspond to the actual values in human larynx.

### 3. Constant solutions and Hopf bifurcations

The system of equations (2.6) is of the form

$$f(Z, \eta) = 0, \quad (3.1)$$

where:  $Z^T = [X, Y, P]$  is the vector of the sought solutions and  $\eta^T = [C, K_x, K_D, X_0, K_{xy}, K_s, S, C_s, E, K_y, Q]$  - the vector of parameters.

Generally, nonlinear systems of algebraic equations (3.1) may only be solved numerically. To this end, the Newton method will be used (see e.g. [19,20]). When the first approximation of the exact solution  $Z_0$  is known, the final solution may be determined very accurately. For the approximate value of the solution  $Z_0$ , the equation (3.1) is not identically satisfied and the solution is determined with an error  $\Delta Z_0$ . Newton's method consists of the substitution of the nonlinear system of equations (3.1) for the linear nonhomogeneous system of equations at every consecutive point determined by consecutive iterations. Solving it, the consecutive errors  $\Delta Z_0$  which finally approach 0 are determined.

Linearization  $f(Z)$  in the neighbourhood of  $Z_0$  results in

$$f(Z) = f(Z_0) + \left. \frac{\partial f(Z)}{\partial Z} \right|_{Z_0} \Delta Z. \quad (3.2)$$

The correction of the solution is equal to

$$\Delta Z = F^{-1} \Big|_{Z_0} f(Z), \quad (3.3)$$

where:

$$F = \frac{\partial f}{\partial Z}, \quad f(Z_0) = 0.$$

Generally, we may present the iteration scheme of Newton method as

$$Z^{i+1} = Z^i - F^{-1} \Big|_{Z^i} f(Z^i). \quad (3.4)$$

Practically, we do not invert the matrix  $F$  in the equation (3.4), but we solve the nonhomogeneous system (3.2) and having the solution  $\Delta Z^i$ , we obtain the improved solution

$$Z^{i+1} = Z^i - \Delta Z^i.$$

The iterations are performed until the desired accuracy is achieved. In order to estimate the stability of the state of equilibrium, we reduce the system of equations (2.6) to the equivalent system of equations of the first order

$$\dot{Z} = h(Z, \eta), \quad (3.5)$$

where:

$$Z^T = [X, \dot{X}, Y, \dot{Y}, P].$$

From the equation (3.5) we obtain the variation equations

$$\dot{Z} = H \Delta Z, \quad (3.6)$$

where the constant Jacobian matrix  $H$  is taken at  $(\dot{Z}, Z, \eta) = (\dot{0}, Z_0, \eta)$  and  $Z_0$  is the vector of equilibrium points. The eigenvalue problem

$$(\lambda I - H)\xi = 0. \quad (3.7)$$

yields the five eigenvalues and corresponding eigenvectors. As a result of computer calculations, these values are obtained by reduction of the real matrix to the Hassenberg form. Eigenvectors are normalized in the way that the sum of squares of moduli of the elements is equal to 1 and the element of the largest modulus is real. This ensures that real eigenvalues have real eigenvectors. Cronjaeger showed, using an analytical method, that in this case neither the real positive eigenvalue nor  $\lambda = 0$  exist. The matrix  $H$  possesses only the negative of conjugate complex eigenvalues. The system (3.6) has two couples of complex conjugate solutions

$$\Delta z_s = \xi_s e^{\lambda_s t},$$

which have the real form

$$\begin{aligned} \Delta z_s &= c_s e^{\delta_s(\tau - \tau_s)} \{ \cos \omega_s(\tau - \tau_s) \operatorname{Re} \xi_s + \\ &\quad - \sin \omega_s(\tau - \tau_s) \operatorname{Im} \xi_s \}, \\ \lambda_s &= \delta_s + i\omega_s, \quad \delta_s = \operatorname{Re} \lambda_s, \quad \omega_s = \operatorname{Im} \lambda_s, \end{aligned} \quad (3.8)$$

where  $c_s$  and  $\tau_s$  are the constants of integration.

In numerical calculation the Newton method converges quickly even if the first approximation of the sought constant solutions diverges considerably from accurate values. In the case when one of the damping coefficients  $\delta_i$  changes its value from the minus one through 0 and assumes the positive value (the other damping coefficients are negative), Hopf bifurcation ([21,22]) takes place and the new periodic solution of the frequency  $\omega_s$  occurs.

For the arbitrarily selected fixed parameters  $K_x = 1$ ,  $K_D = 0.001$ ,  $X_0 = 0.6$ ,  $K_{xy} = 0.3$ ,  $K_s = 0.001$ ,  $C_s = 0.5$ ,  $E = 1$ ,  $K_y = 0.9$ , numerical calculations were performed.

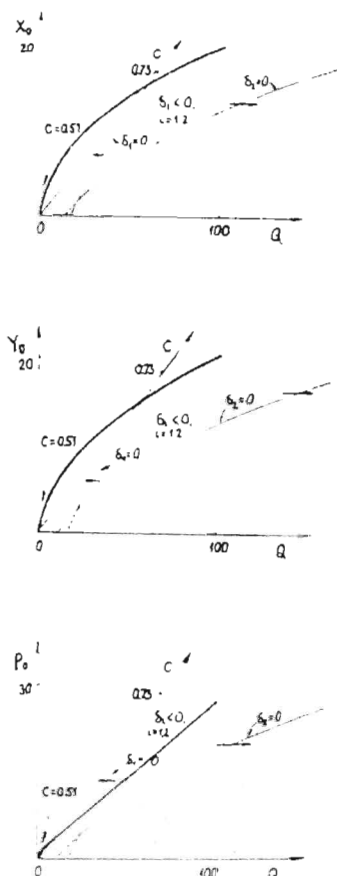


Fig. 2. States of equilibrium of vocal cords marked with broad solid line obtained from the system of equations (2.6) with the use of Newton's method

The diagrams in fig.2 present results being obtained. In the plane of the para-



parameters  $C$  and  $Q$ , the limit curves of the loss of stability for constant solutions were determined. At the arbitrary point of one of the curves  $\lambda_{1,2} = \pm i\omega$  and, after Malkin [23], this case belongs to the critical ones. This is a boundary point separating the stable and unstable steady-state solutions areas. The occurrence of Hopf bifurcation was indicated in the figure by direction arrows. The constant stable solution, e.g. for the determined value  $C$ , after passing the critical value, loses its stability and the new periodic solution appears. Let's determine the eigenvalues as  $\lambda_{1,2} = \delta_1 \pm i\omega_1$ ,  $\lambda_{3,4} = \delta_2 \pm i\omega_2$ ,  $\lambda_5 = -\gamma$ , where  $\gamma > 0$ . The real and imaginary parts of the eigenvalues depend on the parameters  $D$ ,  $Q$  i.e.  $\delta_i(C, Q)$ ,  $\omega_i(C, Q)$ ,  $i = 1, 2$ . On each of the boundary curves, one of the values,  $\delta_i$ , is equal to zero. In fig.2, the limits of the loss of stability were marked by the solid line. For the set of parameters  $C$ ,  $Q$  lying between these two curves (where  $\delta_i < 0$ ), the constant solutions  $Z_0$  are stable. At the point of the two curves intersection, there exists a pair of imaginary coupled eigenvalues and for the parameters  $C$ ,  $Q$  lying below this point there appears a torus with two frequencies. In this case, the solution may be periodic if only  $k\omega_1 = l\omega_2$ , where  $k$  and  $l$  are integers. The limits of the loss of stability were determined within the damping sphere  $0.51 < D < 0.73$ , which corresponds to the real damping values of the human vocal cords. On the basis of numerical calculations, the influence of some essential dimensionless parameters on the position of the loss of stability limits will be considered.

#### 4. Influence of the intensity of the flow $Q$ and the position of the cartilage $X_0$

According to fig.3, for the parameters set lying above the marked line, only steady state solutions are possible. Vocal cords are in equilibrium state. When parameter  $C$ , crosses after all these curves with increased damping (for fixed  $X_0$  and  $Q$ ), the previously stable equilibrium becomes unstable and a new periodic solution emanates from Hopf bifurcation. If  $X_0 \leq 1$  i.e. the glottis is closed, the vibration can easily appear, particularly if the values of intensity of the air flow  $Q$  are low. As the parameter  $X_0$  grows, the vibrations take place only for low values of damping  $C$ . Let us consider the fixed value  $C$  and  $X_0$  and suppose that for a small value of  $Q$  the vocal cords oscillate. Then, with an increase of  $Q$  when the solid line is crossed (fig.3a), the vibrations suddenly stop.

For  $X_0 > 1$ , i.e. when the glottis is open, the situation radically changes. For the low values of  $Q$ , the vibrations may take place only at low values of damping  $C$ . Practically it means, that for real human damping ( $0.5 < C < 1$ ) the vibrations can appear only for values of  $Q$  large enough. Considering, for the fixed values of  $Q$  and  $X_0$  the behaviour of the system when the coefficient  $C$  decreases, starting with a very high value. At a certain value  $C_1$  we will pass the limit of the loss of

(a)

(b)

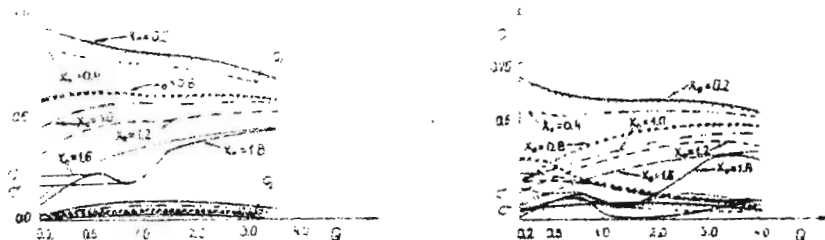


Fig. 3. Limits of the loss of stability of equilibrium of the vocal cords in the space of parameters  $C$ ,  $Q$ ,  $X_0$ . The other parameters:  $K_E = 1$ ,  $K_D = 0.001$ ,  $K_{xy} = 0.3$ ,  $K_s = 0.0001$ ,  $C_s = 0.5$ ,  $E = 1$ . (a)  $K_Y = 0.9$ , (b)  $K_Y = 0.6$

stability means that  $\delta_1 \geq 0$ . Continuing the changes to the lower damping  $\zeta$  we come across another line marked in the figure. Having crossed it we have  $\delta_1 > 0$ , and  $\delta_2 > 0$ . The frequencies corresponding to these values ( $\delta_i$ ,  $i = 1, 2$ ) are equal to  $\omega_1$  and  $\omega_2$  respectively, with  $\omega_1 < \omega_2$ . In the fig.3 it is shown that with the growth of the value of  $X_0$ , two marked in the same way curves being limits of stability approach each other and at certain values of parameters they may cross. It means the frequency of the vibrations changes (change of voice register) and this case is presented in fig.3b. As can be seen in this figure, such a variation of frequency may also accompany the change of parameter  $X_0$  (other parameters are fixed)

For a very high value of  $X_0$  ( $X_0 = 1.8$ ), in a certain sphere of changes of the parameter  $Q$ , strong nonlinear effects are observed. The growth of  $Q$  is accompanied first by the rapid decrease and then the growth of the limit of stability. If only  $C'' < C < C'''$  and the other parameters are fixed, then three different values of  $Q$  correspond to the same value of  $C$ .

## 5. Influence of the parameter $E$

In fig.4, the diagrams of the limits of the loss of stability in the space of parameters  $C$ ,  $E$ ,  $Q$ , are presented. Similarly as in the above case, the rapid change of vibration frequency is possible. The change of vibration frequency from the low one to the higher one takes place when for the fixed value  $Q$  ( $E$ ) the parameter  $E$  ( $Q$ ) will exceed a certain critical value. Some nonlinear effects introduced by the nonlinearity of the Duffing type ( $K_D \neq 0$ ) are evident. The curve  $C(Q)$  being

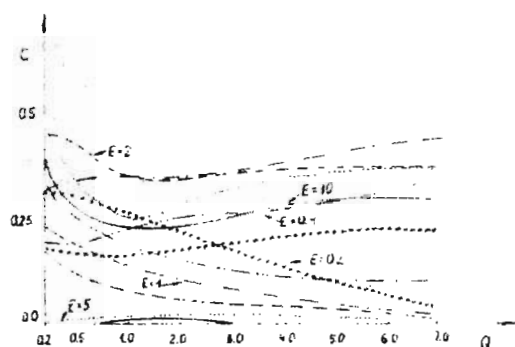


Fig. 4. Damping effect on the limits of the loss of stability against the intensity of flow  $Q$  and the surface of the vocal cord  $E$ . The other parameters:  $K_x = 1$ ,  $K_D = 0.001$ ,  $K_s = 0.001$ ,  $C_s = 0.5$ ,  $K_y = 0.3$ ,  $K_{xy} = 0.3$ ,  $X_0 = 0.4$

the limit of the loss of stability (for the fixed value  $E$ ) first decreases, achieves the minimum, and with further growth of  $Q$ , increases monotonically. Additionally, numerical calculations have proved that frequency of the vibrations is essentially influenced only by two parameters: the linear stiffness  $K_y$  and the parameter  $E$ . The growth of these two parameters increases the frequency of vibration.

#### 6. Influence of elastic coupling $K_{xy}$ and parameter $K_D$

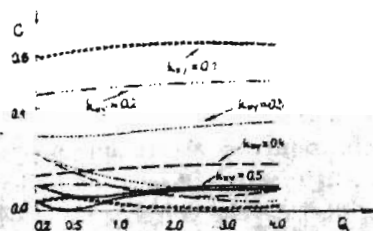


Fig. 5. Damping influence on the limits of the loss of stability versus the coefficient of elastic coupling of vibrations  $K_{xy}$  and the intensity of the flow  $Q$ . The other parameters:  $K_x = 1$ ,  $K_D = 0.001$ ,  $K_s = 0.001$ ,  $C_s = 0.5$ ,  $K_y = 0.3$ ,  $E = 1$ ,  $X_0 = 0.6$

For small values of  $K_{xy}$  (see fig.5) the jump of the frequency of vibrations at the points of the loss of stability is not possible (lines marked in the same way in the figure do not cross). This effect takes place only in a certain narrow interval of variations of this coefficient ( $0.35 < K_{xy} < 0.45$ ). Moreover, with the growth

of this coefficient, the position of the limit of the loss of the stability decreases quickly. This means that the vibrations easily appear at small values of  $K_{xy}$ . The influence of the parameter  $K_s$  on the position of the limits of the loss of stability is presented in the figure 6, however this influence has an insignificant effect on the limit positions.

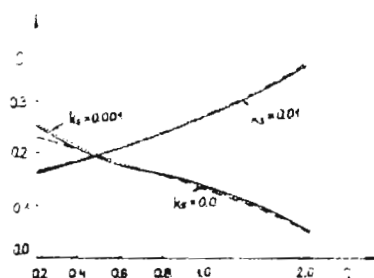


Fig. 6. Damping on the limits of the loss of stability versus the stiffness coefficient  $K_s$  and the flow intensity  $Q$ . The other parameters:  $K_x = 1$ ,  $K_D = 0.001$ ,  $K_y = 0.3$ ,  $E = 1$ ,  $X_0 = 0.6$ ,  $K_{xy} = 0.4$ ,  $C_s = 0.5$

## 7. Calculations of periodic solutions

In order to determine periodic orbits occurring as a result of Hopf bifurcation, we shall introduce the dimensionless frequency  $\omega$  and the relative time  $\tau = \omega t$  into the system of equations (2.6).  $\omega$  enters the equations as a fixed parameter when examining special solutions. The family of periodic solutions  $z(t)$  of a period  $T$  corresponds to the family of periodic solutions  $z(\tau, \omega)$  of a period  $2\pi$ . The method of determining periodic orbits in the autonomous initial system of equations (2.6), due to the introduction of the parameter  $\omega$ , is analogous to the one applied in non-autonomous systems. A new periodic solution is now sought with the a priori known period  $2\pi$ . The corresponding frequency  $\omega$ , however, is numerically determined. Since the analysed system of equations is smooth, its linearization can be easily performed with the assumption that disturbances of the variation  $\Delta z$  are small. Then we apply the theory of linear differential equations with periodic coefficients (see e.g. [23,24]).

For the determination of periodic solutions we shall use Newton's method outlined in chapter 3. The approximate values of the vector  $Z^T = [X, \omega, Y, \dot{Y}, P]$  being known, we perform the numerical integration of the analysed system of equations in the time interval 0 to  $2\pi$  (for  $\dot{x} = 0$ ). Then, the shooting method is used and the values of coordinates for the time  $2\pi$  are considered as new initial

conditions. The use of the Newton method makes the differences between thus iteratively determined solutions, approach 0. The desired precision having been achieved, the calculations are interrupted. Calculations have proved that as far as the numerical integration methods are concerned, the procedures basing on the Runge-Kutta method are not sufficiently accurate. During vibrations, as  $X$  tends to zero can not become negative, an infinitely high repulsive force arises. In the equations (2.6) the term following the coefficient  $K$ , describes it. However, the coordinate  $X$  assumed negative values while these methods were used. For calculations, then, a variable order, variable step Gear method was applied and the calculations were carried out with the step  $10^{-8}$  and with double precision.

Let's now consider two consecutive, iterative steps:

$$g = z(z_0, \tau_0), \quad (7.1)$$

$$h = z(z_0, \tau_0 + 2\pi), \quad (7.2)$$

where  $z_0$  is a certain approximation of the sought values.

If for a certain  $z_0$  the difference  $g - h \equiv 0$ , then  $z_0$  determines the solution of the problem.  $K$ -iteration step determined by Newton's method allows as to determine the correction  $\Delta z^k$  from the equation

$$(I - J^{(k)})\Delta Z^{(k)} = Z^{(k)}(Z_0, \tau_0 + 2\pi) - Z^{(k)}(Z_0, \tau_0), \quad (7.3)$$

where:

$$Z^{(k+1)} = Z^{(k)} + \Delta Z^{(k)}.$$

The Jacobian matrix  $J = \partial h / \partial Z$  is numerically determined for  $Z = Z^{(k)}$ . The initial point of Newton's method results from the calculations carried out in chapter three, where also the frequency value  $\omega$  at the critical point during Hopf bifurcation is given. Let  $z^*(\tau)$  be the determined periodic solution and the problem of examination of its stability be reduced to the analysis of the system of equations

$$\Delta \dot{z} = H^* \Delta z, \quad (7.4)$$

where:

$$H^*(\tau + 2\pi) = H^*(\tau)$$

and  $\Delta z$  is the vector of disturbances.

The arbitrary solution of equations (7.4) is

$$\Delta z(\tau) = \Phi(\tau)\Delta Z(0), \quad (7.5)$$

where the matrix  $\Phi(\tau)$  is the fundamental matrix of solutions. According to Floquet theory, the solutions (7.5) fulfill the relationship

$$\Delta z^F(\tau + 2\pi) = \sigma \Delta z^F(\tau), \quad (7.6)$$

where  $\sigma$  are the characteristic multipliers.

Then the problem of the analysis of the stability of solutions reduces to the eigenvalue one

$$\Phi(2\pi)b = \sigma b, \quad (7.7)$$

with the characteristic equation

$$\det(\Phi(2\pi) - \sigma I) = 0. \quad (7.8)$$

Equation (7.8) allows for the calculation of characteristic multipliers  $\sigma$ , and from the equation (7.7), the corresponding eigenvectors  $b$ , can be obtained. Since  $\Phi(2\pi)$  is a real matrix, the characteristic multipliers are real or complex coupled ones. Numerical calculations make it easy to determine these values, thus to estimate the stability of the previously found periodic solutions. Such a formulation of the problem allows for a complete insight into the neighborhood of the known periodic solutions. One may also easily observe the behaviour of solutions while parameters are being changed. The main advantages of such a formulation is however, the possibility of observing the changes of stability of analysed solutions determination of the bifurcation points or the possibility of finding new solutions arising after bifurcations.

Because the system (2.6) is autonomous, a phase condition  $\dot{x} = 0$  is prescribed in order to fix the unknown frequency  $\omega$ . If the solution is unfavorably stated (not uniquely solvable for  $z(\omega)$ ), an exchange of the fastest varying values of  $z_l$  removes the numerical difficulties ( $z_l$  is chosen,  $\omega$  calculated).

A similar method, based on the Urabe procedure [25,26] was already successfully applied to the computation of bifurcation points and periodic orbits of the rotor vibrations by Brommundt [27,28].

## 8. Examples of self-excited periodic oscillations

The theoretical results of the previous section will now be used to obtain the branches of self-excited oscillations. The calculations were carried out for damping of  $C = 0.61$ , which corresponds to the real damping coefficient of the human vocal cords. Numerical integration yields the fundamental matrix eigenvalues of which are the characteristic multipliers. As the system of equations (2.6) is autonomous, one of the characteristic multiplier must be equal to 1. If the other four eigenvalues are inside the unit circle of the complex plane, then the considered periodic orbit is stable. If one real, or the pair of complex conjugate eigenvalues crosses the unit circle, branching of the periodic solutions occurs. Following Arnold [29] one can expect birth or annihilation of the limit cycle, transcritical or pitchfork bifurcation if one eigenvalue crosses the unit circle at  $+1$ , period doubling if one eigenvalue

crosses this circle at -1 and finally nonlinear resonance or bifurcation into torus if a pair of eigenvalues with nonzero imaginary parts crosses the unit circle.

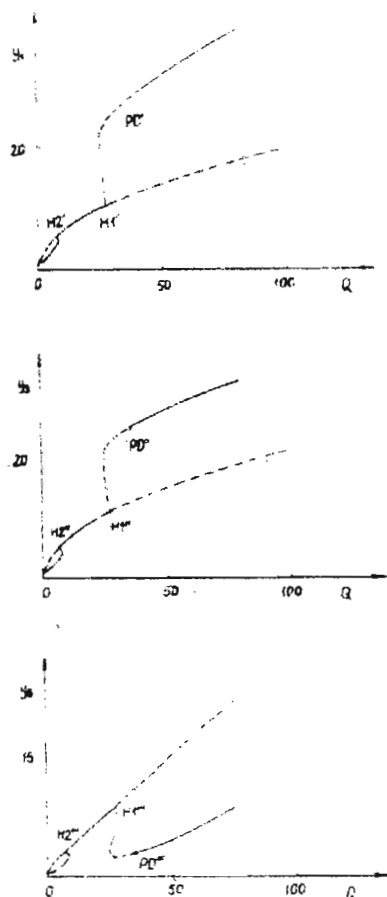


Fig. 7. Bifurcations of periodic solutions determined by the shooting method and Newton's procedure with marking the bifurcation points for the parameters:  $K_x = 1$ ,  $K_D = 0.001$ ,  $X_0 = 0.6$ ,  $\bar{A}_{xy} = 0.3$ ,  $K_s = 0.001$ ,  $C_s = 0.5$ ,  $E = 1$ ,  $K_y = 0.9$

Figure 7 shows the branching diagram for  $C = 0.61$  and  $X_0 = 0.6$ . There are two Hopf bifurcation points from which periodic orbits emanate. From the point H2 emanates a stable periodic solution, while from the point H1 an unstable one. The latter becomes stable when, as  $Q$  increases PD (period doubling) point arises. At this point the new subharmonic solution is born.

The exemplary results of calculations of periodic orbits are given in the figures 8 and 9. Generally system of equations (2.6) can be projected on the  $(y_i, y_j)$  planes

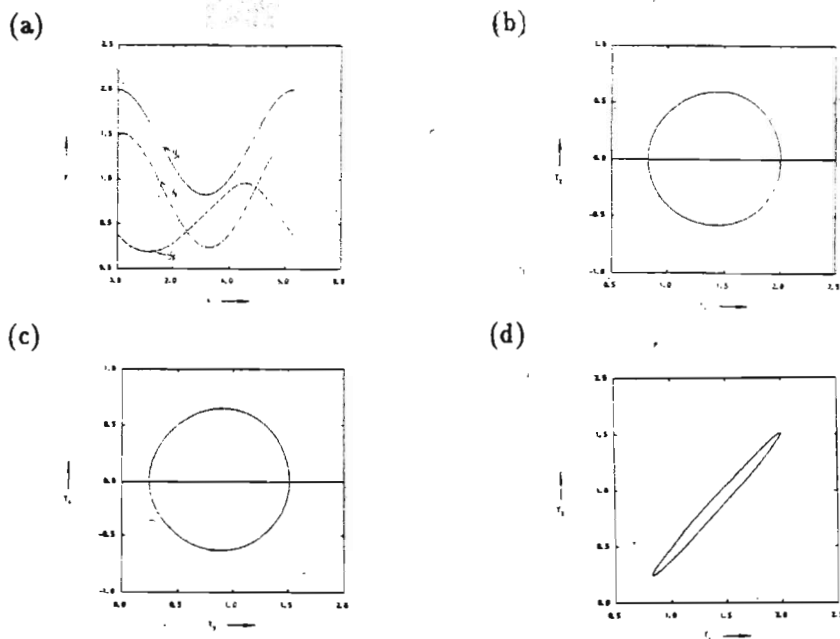


Fig. 8. Periodic motion of the vocal cord for the parameters as in fig.7 with  $C = 0.61$  and  $Q = 0.282$ : (a) time history; (b) phase portrait  $y_2(y_1)$ ; (c) phase portrait  $y_4(y_3)$ ; (d) trajectory of the vocal cord  $y_3(y_4)$

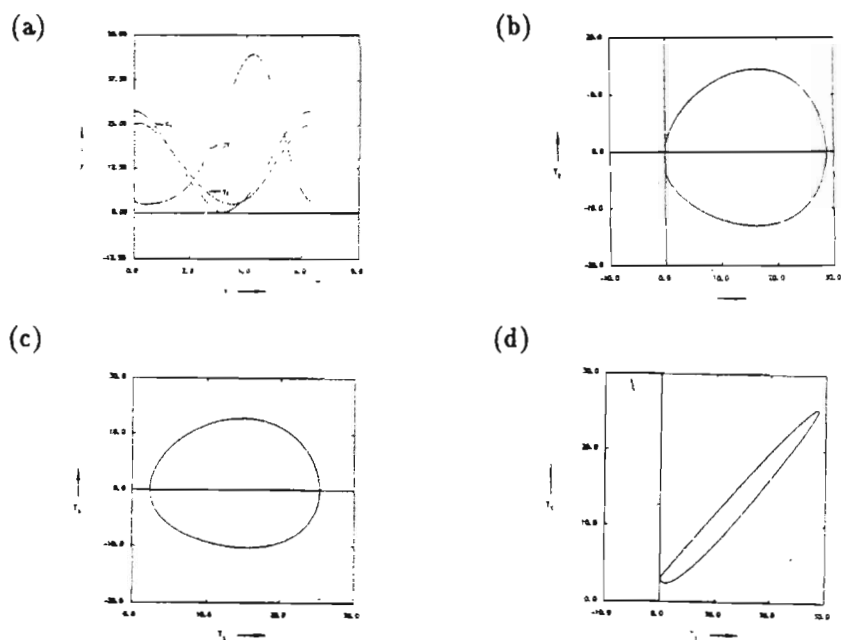


Fig. 9. Periodic motion of the vocal cord for the parameters as in fig.7 with  $C = 0.61$  and  $Q = 40$ : (a) time history; (b) phase portrait  $y_2(y_1)$ ; (c) phase portrait  $y_4(y_3)$ ; (d) trajectory of the vocal cord  $y_3(y_1)$



where  $i, j = 1, \dots, 5$  in ten different ways. In the figures are presented only three-two phase portraits  $y_2(y_1)$ ,  $y_4(y_3)$  and the trajectory of the vocal cord  $y_3(y_1)$ . The new variables  $y_i$  are defined:  $y_1 = X$ ,  $y_2 = \dot{X}$ ,  $y_3 = Y$ ,  $y_4 = \dot{Y}$ ,  $y_5 = P$ .

Let us consider the first one of the periodic orbits which belongs to the left branch in fig.7 ( $Q = 0.282$ ). To the small value of the flow intensity  $Q$  corresponds a relatively small value of pressure  $P$ . In this case the impact phenomena between vocal cords do not appear. Amplitudes of horizontal and vertical vibrations of the vocal cord are approximately of the same order. The nonlinearities of the system, because of the small amplitudes of vibrations, cause small deformations of the time histories and phase portraits. The situation changes however, when the periodic orbit belongs to the right bifurcation branch in fig.7. For large values of  $Q$  ( $Q = 40$ ) the impact phenomenon is observed (fig.9). It is clearly visible that for  $y_1$  close to zero, the phase curve  $y_2(y_1)$  has a vertical part. For these reasons the standard Runge-Kutta methods are not sufficiently accurate for integration of the stiff equation system (2.6). A variable order variable step Gear method with the small step was used and integrations were carried out with double precision. The amplitudes of vibrations are wide and the deformations of phase portraits and time histories are clearly visible.

Finally, let us consider the behaviour of the vocal cord for the parameters as in fig.4 and for  $E = 0.2$  and  $Q = 0.5$ . Starting with high values of damping  $C$  and then decreasing them we cross the first limit of stability and after Hopf bifurcation the limit cycle appears. It is presented in fig.10, for  $C = 0.28666$  ( $\omega = 0.5517$ ). With the further decrease of damping we cross the second limit of stability and the another bifurcation cycle emanates from the second Hopf bifurcation point. It is presented for  $C = 0.07321$  ( $\omega = 1.07674$ ) in fig.11. As can be seen from these figures, two presented periodic orbits differ from each other not only in the frequency, but also in the normal modes (see the trajectory  $y_3(y_1)$ ) of the vocal cord.

## 9. Concluding remarks

The numerical analysis of differential equations governing the dynamics of the vocal cords enables us to draw the following conclusions.

1. For the arbitrarily chosen parameter set (see fig.2) there exist two limits of the loss of stability on the parameter plane  $(C, Q)$  which intersect each other. For the parameters set  $C, Q$  lying between these two limits (where  $\delta_i < 0, i = 1, 2$ ) the steady-state solutions are stable, while in the other region after Hopf bifurcation these solutions become unstable and periodic orbits appear. The region of stable steady state solution becomes wider as damping  $C$  and intensity of air flow  $Q$  are increased. If for a certain value  $Q_0$  the vocal cords are in the state of equilibrium,

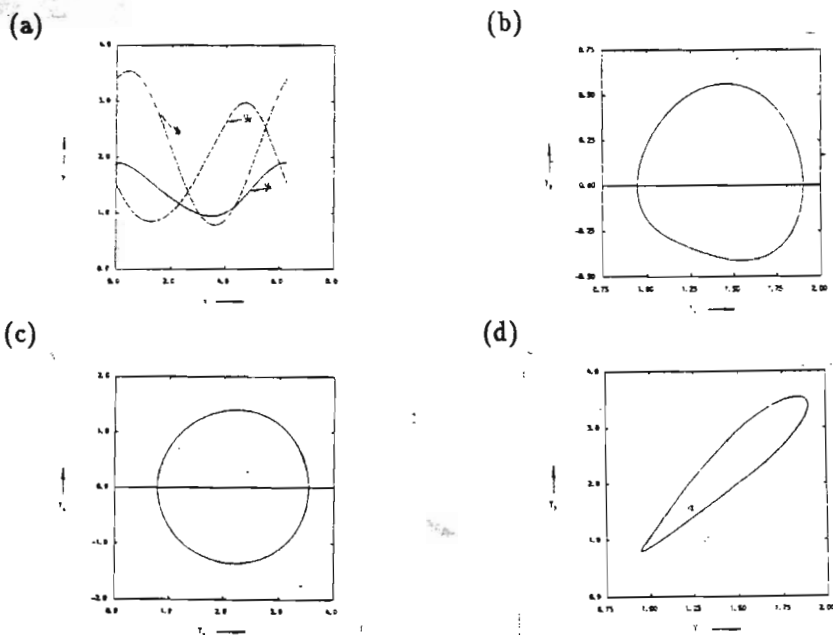


Fig. 10. Periodic motion of the vocal cord for the parameters as in fig.4 and additionally  $E = 0.2$ ,  $Q = 0.5$ ,  $C = 0.28666$ : (a) time history; (b) phase portrait  $y_2(y_1)$ ; (c) phase portrait  $y_4(y_3)$ ; (d) trajectory of the vocal cord  $y_3(y_1)$

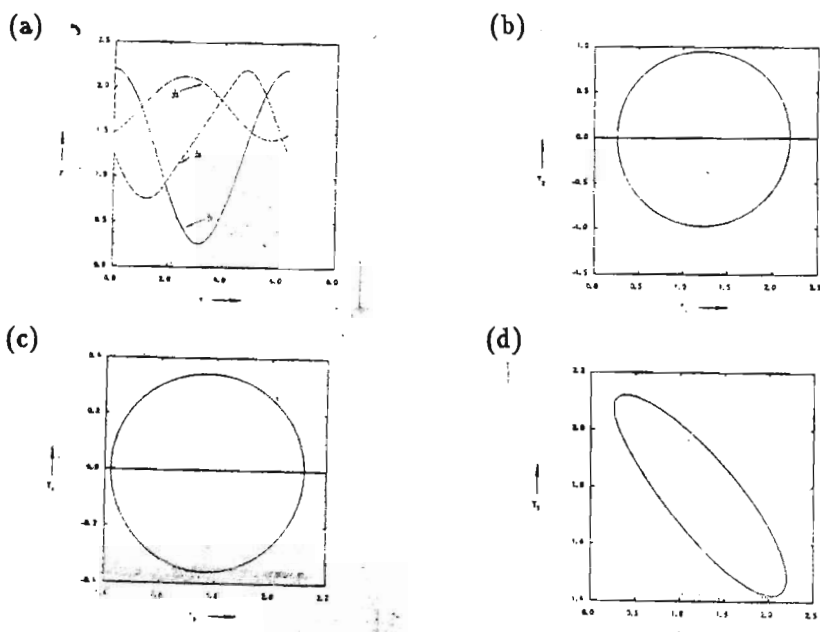


Fig. 11. Periodic motion of the vocal cord for the parameters as in fig.10 and  $C = 0.07321$ : (a) time history; (b) phase portrait  $y_2(y_1)$ ; (c) phase portrait  $y_4(y_3)$ ; (d) trajectory of the vocal cord  $y_3(y_1)$

both the increasing and decreasing of  $Q$  cause the appearance of periodic orbits after Hopf bifurcation (with different frequencies).

2. As it can be seen in the fig.2, where bifurcation curves are crossed, there appear two frequency vibrations. Depending on the relationship between these frequencies the motion of the vocal cords may be periodic or quasiperiodic.

3. For the closed glottis ( $X_0 \leq 1$ ) the vibrations occur already at low values of the flow intensity  $Q$ . However, for high values of  $Q$ , for vibrations to take place, damping  $C$  must be low enough. Thus for the given value  $C$ , "breaking" of vibrations may be caused by the growth of  $Q$  (fig.3).

4. When the glottis is open  $X_0 > 1$  the vibrations may arise only for high values of  $Q$ .

5. Changing  $Q$  or  $X_0$  to a certain extent causes jumping from one voice register to the other one possible (fig.3b).

6. As shown in fig.10 and fig.11, the change of voice register is also possible when the parameters  $Q$  and  $E$  are varying (fig.4). Voice registers differ first of all in frequency and as it is proved by numerical calculations also in the corresponding model forms of vibrations.

7. Parameter  $K_y$  and  $E$  exert considerable influence on the vibration frequency and in this way on the sound. In particular, their growth brings about the growth of vibration frequency.

8. In certain intervals of the coefficient  $K_{xy}$  the change of voice register is also possible. Vibrations may occur only at low values of this coefficient (fig.5).

9. The steady - state solutions equilibrium position of the vocal cords lose their stability with the change of intensity of the flow  $Q$ . Then with the further changing of this parameter the stability of these solutions changes and new sub-harmonic solutions appear (fig.7).

#### Acknowledgement

The author would like to thank E.Brommundt for helpful discussion relating to this investigations. This work was supported by Alexander von Humboldt Foundation.

#### References

1. CRONJAEGER R., *Model of the sound generation in a human larynx*, PhD Thesis, Braunschweig 1978 (in German)
2. VAN DEN BERG JW., ZANTEMA J.T., DOORNEUBAL P., *On the air resistance and the Bernoulli effect of the human larynx*, J. Acoust. Soc. Amer. 29, 626-631, 1957
3. VAN DEN BERG JW., *On the myoelastic-aerodynamic theory of voice production*, Nat. Bull. Inst. Hlth. Bull. 14, 6-12, 1958
4. VAN DEN BERG JW., *Modern Research in Experimental Phoniatrics*, Folia Phoniat. 14, 81-149, 1962

5. FLANAGAN J.L., *Source-system interaction in the vocal tract*, Ann. New York Acad. Sci., 155, 9-17, 1968
6. FLANAGAN J.L., LANDGRAF L.L., *Self-oscillating source for vocal-tract synthesizers*, IEEE Trans. Audio Electroacoust. AU-16, 57-64, 1968
7. FLANAGAN J.L., CHERRY L., *Excitation of vocal tract synthesizers*, J. Acoust. Soc. Amer. 45, 764-769, 1969
8. FLANAGAN J.L., *Speech Analysis, Synthesis and Perception*, New York, 1972
9. BENNINGHOFF-GOERTTLER, *Handbook of the Human Anatomy*, München, 1967
10. LULLIES H., *Physiology of Voice and Speech*, Berlin, 1953
11. LUCHCINGER R., *Physiology of Voice*, Folia Phoniat., 5, 58-128, 1953
12. ZOLLNER F., *Neck-Therapeutics of the Neck - Nose and Ears*, Stuttgart 1974 (in German)
13. ROHEN J.W., TAUTZ K., HECKEMANN L., *New Findings about the Anatomic Basis of Voice Formation*, Med. Welt 19, 1099-1102, 1969 (in German)
14. WUSTROW F., *Characteristics and Functions of the Human Musculus Vocalis*, Z. Anat. u. Entw. Gesch. 116, 506-522, 1952 (in German)
15. WUSTROW F., *Active or Passive Oscillations of the Vocal Cords*, Z. Laryng. Rhinolog. Otol. 32, 572-577, 1953
16. LULLIES H., *About the Origin of the Sound of Whistling. Additional Information to Vocal Questions*, Arch. 211, 373-390, 1925 (in German)
17. LOTTERMOSER W., *Lectures about Sound Formation in Musical Instruments and Speech*, Naturwiss. 37, 302-308, 1950 (in German)
18. DAMSTE P.H., *The Vibrations of the Vocal Cords Compared with Vibrations of the Trombone*, J. Otol. Rhinol. Laryng. XV, 395-396, 1966 (in French)
19. STOER J., BULIRSCH R., *Introduction to Numerical Analysis*, Springer Berlin 1978
20. TORNING W., *Numerical Mathematics for Engineering and Physics*, Band 1, 2, Springer Berlin 1979
21. J.E. MARSDEN J.E., MCCracken M., *The Hopf Bifurcation and its Application*, Applied Mathematical Sciences 19, Springer New York, 1976
22. HASSARD B.D., KAZARINOFF N.D., WAN Y.H., *Theory and Applications of Hopf Bifurcation*, Cambridge University Press, 1981
23. MALKIN I.G., *Some Problems in the Theory of Nonlinear Oscillation*, Moscow, 1956 (in Russian)
24. IAKUBOWICH V.A., STARZHINSKI V.M., *Linear Differential Equations with Periodic Coefficients and Their Applications*, Moscow, Nauka, 1972 (in Russian)
25. URABE M., *Galerkin's Procedure for Nonlinear Periodic Systems*, Arch. Rat. Mech. Anal. 20, 120-152, 1965
26. URABE M., REITER A., *Numerical Computation of Nonlinear Forced Oscillations by Galerkin's Procedure*, J. Math. Anal. Appl. 14, 107-140, 1966
27. BROMMUNDT E., *On the Numerical Investigation of Nonlinear Periodic Rotor Vibrations*, Dynamics of Rotors, IUTAM - Symposium in Lyngby (Denmark) 1974, Springer Verlag, Berlin, Heidelberg, New York 1975

28. BROMMUNDT E., *Bifurcation of Self-Excited Rotor Vibrations*, International Conference on Nonlinear Vibration, Akademie-Verlag Berlin 123-134, 1977
29. ARNOLD V.I., *Geometrical Equations*, New York, Heidelberg, Berlin Springer 1983

### Streszczenie

Praca przedstawia systematyczną globalną analizę numeryczną dynamiki ludzkich strun głosowych, opisaną układem równań różniczkowych nieliniowych zwyczajnych piątego rzędu. Najpierw wyznaczono w przestrzeni parametrów położenia równowagi strun głosowych. Następnie, rozwiązując problem warunków brzegowych znaleziono orbity okresowe powstające z położenia równowagi w wyniku bifurkacji Hopfa. Stateczność i możliwe bifurkacje tych orbit śledzone były poprzez obserwację zmian wartości mnożników charakterystycznych.

Zilustrowano wpływ parametrów na pojawienie się dźwięku okresowego jedno- i dwuczęściowego lub quasiokresowego. Ponadto przedyskutowano zjawisko zmiany rejestru głosu.

*Praca wpłynęła do Redakcji dnia 16 stycznia 1990 roku*